Proc. of the 32nd International Symposium on Shock Waves (ISSW32)
doi:10.3850/978-981-11-2730-4_0376-cd
Copyright © 2019 ISSW32. All rights reserved.

The Aerodynamic Performance of an Aerofoil in Tri-sonic Ground Effect

S. R. Morrow, H. Roohani, B. W. Skews, I. Gledhill
Flow Research Unit, University of the Witwatersrand, 1 Jan Smuts Avenue, Braamfontein, Johannesburg, 2000, South Africa
B. J. Evans
College of Engineering, Swansea University, Bay Campus, Fabian Way, Skewen, Swansea, SA1 8EN, United Kingdom

Sean Morrow: sean.morrow@students.wits.ac.za

Abstract Inspired by the world land speed record vehicles, the Thrust and Bloodhound Supersonic Cars (SSC); this investigation considers the influence of ground effect and acceleration on the aerodynamic performance of an aerofoil accelerating in ground effect from subsonic to supersonic speeds. Using Fluent as the computational fluid dynamic solver, a steady state analysis of the RAE 2822 aerofoil at two different ground clearances was used to evaluate the influence of ground effect. The effects of acceleration were considered by comparing the steady state results against transient models with extreme accelerations of 175g. The aerodynamic performance and shock wave development were analysed from Mach 0.20 to Mach 2.00. The analysis revealed that both ground effect and acceleration impact on the shock wave development and propagation through the flow. An increase in ground effect proved to dramatically improve the supersonic lift performance of the aerofoil and alter the shock system that forms below the aerofoil. The extreme acceleration revealed that transient flow lags behind the steady state flow and the lift and drag performance of the aerofoil are impacted differently by the flow history and inertia of the fluid. Flow history causes the transient lift performance to lag behind the steady state performance and has minimal effect on the drag performance. The inertia of the fluid resists the acceleration of the aerofoil and significantly increases the subsonic drag. These two effects then combine to substantially reduce the aerodynamic efficiency of the transient aerofoil.

1 Introduction

In 1997, the Thrust SSC set the current world land speed record of 763 mph (1228 km/h) [1]. In order to break this record, the Bloodhound SSC will need to accelerate and decelerate at up to 3 g and -3 g, to reach its top speed and then stop safely. This brings up the question of how rapid acceleration and deceleration affects the shock formation on lifting bodies in transonic and supersonic ground effect.

The focus of this preliminary research is to investigate the aerodynamic performance of an aerofoil accelerating in subsonic, transonic and supersonic (tri-sonic) ground effect. Two important factors to consider are the transient effects of acceleration and the influence of ground effect. Transient flow history and fluid inertia effects have been shown to respectively decrease the subsonic lift and increase the subsonic drag of an aerofoil as it accelerates [2]. Acceleration and deceleration also impacts on the formation and dissipation of shock waves coming off an aerofoil traveling at transonic and supersonic speeds [3]. Ground effect has been shown to enhance both the lift and down force being produced by an aerofoil [4].

In a previous computational study, the effects of acceleration were determined by comparing steady state and transient models of an inverted NACA 0012 aerofoil [5]. The aerofoil was accelerated from Mach 0.05 to Mach 1.60 at an extreme acceleration of 175 g to reveal that the transient shock wave development lags behind that of the steady state. The main reason for the lag is that the transient flow is unable to fully develop and reach a state of equilibrium. A consequence of this lag or flow history is an average drop in the lift of 9% between the transient and steady state cases. The drop in down force was highest (19%) in the subsonic region, between Mach 0.05 and Mach 0.50.

In this study, the influence of ground effect is considered by reducing the ground clearance of an aerofoil with a constant angle of attack. Extending upon the research done by Doig et al. [6], a tri-sonic speed range is considered, starting at a subsonic speed of Mach 0.05 and ending at a supersonic speed of Mach 1.70. The aerodynamic performance of an RAE 2822 aerofoil is analysed here at two different ground clearances.

2 Numerical Models

As with the NACA0012 case mentioned above, an ANSYS Fluent, non-inertial, implicit, density based solver was used to analyse the impact of ground effect and acceleration on the aerodynamic performance of an RAE 2822 aerofoil. The RAE 2822 aerofoil was modelled with a chord length of 3.05 m and a positive angle of attack of 2.79°. The domain was set with pressure far field boundary conditions 20 chord lengths ahead and behind the aerofoil and 15 chord lengths above the aerofoil. Two different models were created with the wall below the aerofoil set at two different ground clearances: one chord length (h/c = 1) and half a chord length (h/c =0.5). The aerofoil was then kept stationary and the velocity of the flow was applied at the pressure far field boundaries and moving ground wall.. The meshes for both models were constructed using inflation layers and edge sizing on the aerofoil and ground immediately under the aerofoil. The inflation layer on the aerofoil features an initial cell height of 1 x 10^{-5} m, to ensure the boundary layer was accurately modelled. Figure 1, shows the domain, boundary conditions and an example of the meshing technique used to set up each model.

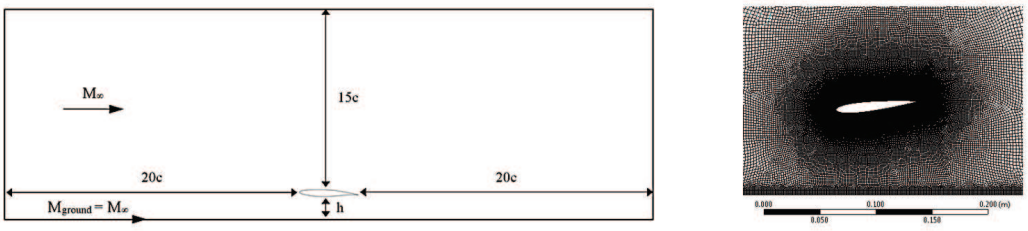

Fig.1 Domain, boundary settings and meshing technique used for all the RAE 2822 aerofoil models

2.1 Validation Models

The above parameters were chosen for the RAE 2822 model to match the models used by Doig et al. [6]. A validation model was run for each ground clearance at a velocity of Mach 0.90, Reynold's number of 6.4 x 10^7 (based on chord length) and compared to the

corresponding RAE 2822 cases run by Doig et al. [6]. In each case, the non-inertial, density based model described above showed a strong correlation with the validated pressure based models used in these cases - as shown in Figure 2.

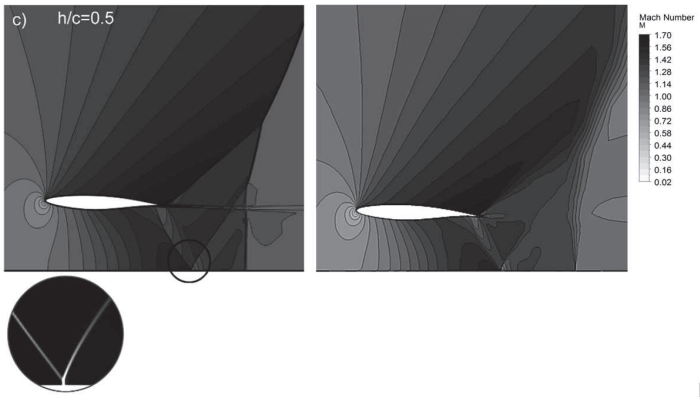

Fig.2 Comparison of the Mach number contours produced by the validation model (right) against existing validated research (left, Doig et al. [6])

2.2 Acceleration Models

Adopting the same parameters and methodology used in the NACA 0012 case, the steady state and transient RAE 2822 models were run from Mach 0.20 to Mach 2.00. Intervals of Mach 0.05 (17.35 m/s) were used between each steady state case, while the transient case was accelerated through the speed range at an extreme rate of 175g (1716 m/s^2). The flow field was accelerated by applying user defined functions at the boundary conditions and source terms throughout the flow field. Time dependent Mach number and velocity functions were used to increase the free stream Mach number at the pressure far field boundaries and the velocity of the moving ground wall. In order to accelerate the flow field uniformly and allow the flow to develop naturally, the acceleration terms in the energy and momentum equations were isolated and applied throughout the flow using user defined energy and momentum source term functions. The steady state simulations are run first for each case and analysed to get an understanding of the accelerating flow field. The transient simulations are then run using the Mach 0.20 steady state results to initialize the flow field. Aerodynamic performance results and contour plots are then recorded, compared and analysed to determine the effects of acceleration on the developing flow field and formation, reflection and interaction of the resulting shock waves. An extreme acceleration has been used in order to fully evaluate the effects of acceleration.

3 Results and Discussion

3.1 Steady State Analysis

The steady state results for the two ground clearance cases were analysed and compared to determine the influence of ground effect on the development of the flow and resulting shock systems. Figure 3 compares the steady state lift performance for the two ground clearances. The increased ground effect leads to a consistent increase in the lift produced

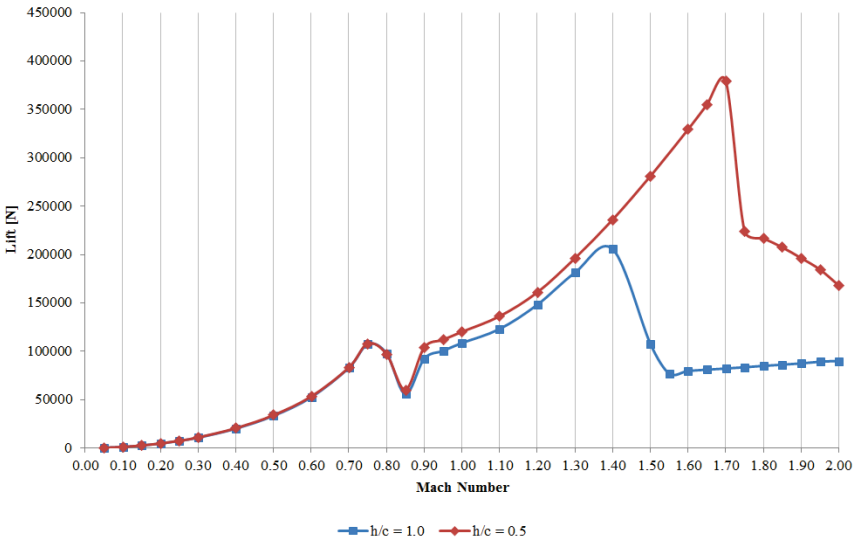

Fig.3 Lift performance curves for an RAE 2822 aerofoil at two different ground clearances: h/c = 1.0 and h/c = 0.5

by the lower h/c = 0.5 aerofoil. For most of the velocity range the lift performance follows the same trend, with the produced lift only varying by an average of 1.9% between Mach 0.20 and Mach 0.80. This difference then grows as shock waves start to form above and below the aerofoil. In both cases, the conditions above the aerofoil are the same and a shock wave develops on the upper surface of the aerofoil at a critical Mach number of Mach 0.55. Initially, the lift increases exponentially, but it then drops between Mach 0.75 and Mach 0.90 as a shock wave forms and moves along the lower surface of the aerofoil - as seen in Figure 4 (a). As the lower shock moves towards the trailing edge of the aerofoil, another shock wave forms at the inflection point of the reflex aerofoil. A small region of subsonic flow forms behind this shock wave and extends to the trailing edge. Figure 4 (b) shows that as the flow reaches the trailing edge it becomes supersonic again and an expansion shock wave comes off the trailing edge. The lower shock waves approach the ground and start to curve as they become normal to the ground. The stronger oblique shock dominates and reflects off the ground. As the flow accelerates, the oblique shock stablises and strengthens while the reflected shock propagates further downstream. Consequently, the shock system under the aerofoil remains fairly constant and the lift increases exponentially up until Mach 1.40. During this period, the influence of ground effect is evident by the lower aerofoil featuring an average increase in lift of 10.6%.

From Mach 1.40 onwards, the results diverge and the average increase in lift is 200%. At Mach 1.70, the produced lift differs by a maximum of 361%. The reason for the divergence in lift can be seen in Figure 5, as the bow shock moves under the h/c = 1.0 aerofoil and reflects off the ground, it disrupts the pressure distribution below the aerofoil. This does not happen in the case of the h/c = 0.5 aerofoil until Mach 1.70, because the lower ground clearance restricts the flow and increases the pressure under the aerofoil. The air flow under the aerofoil has reached the Kantrowitz limit and becomes choked. Therefore, the pressure and density of the air underneath the aerofoil increases and more air is forced to travel over the top of the aerofoil. This effect leads to a greater pressure

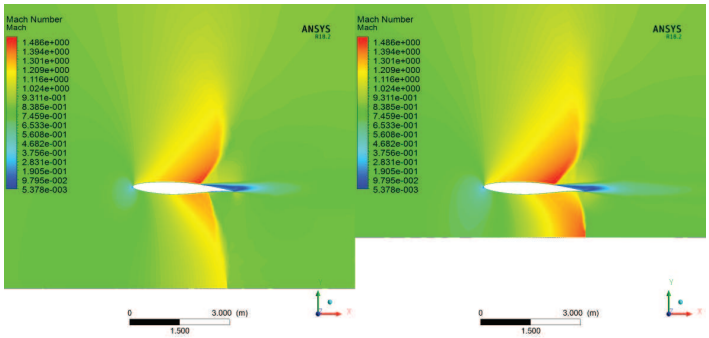

(a) Mach 0.85

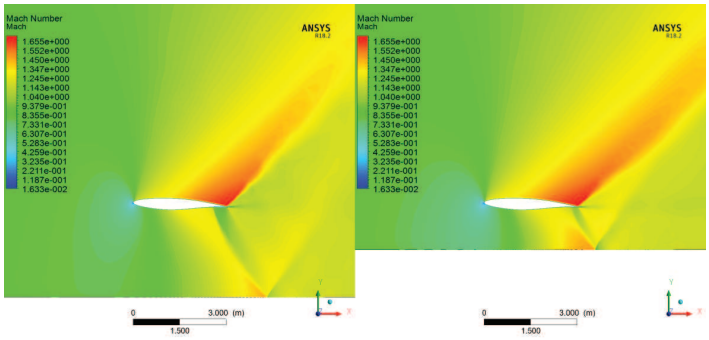

(b) Mach 0.95

Fig.4 Comparison of the h/c = 1.0 (left) and h/c = 0.5 (right) steady state Mach number contour plots at (a) Mach 0.85 and (b) Mach 0.95

differential across the aerofoil and as the flow accelerates, more and more lift is produced. The leading edge stagnation point also moves further down the aerofoil and a large region of high pressure subsonic flow forms under the leading edge of the aerofoil.

Figure 5 shows that, as the free stream velocity approaches Mach 1.70, the bow shock starts to bend as it tries to move under the aerofoil and remain normal to the ground. The curvature of the bow shock continues to increase until it can longer be sustained and the adverse pressure gradient under the aerofoil causes a Mach reflection to occur. At Mach 1.75, the reflected bow shock and increasing upstream pressure disrupts and overpowers the high pressure region and the reflected bow shock propagates under the aerofoil. This shock then reflects between the ground and aerofoil downstream, which further reduces the pressure differential across the aerofoil and adds to the dramatic drop in lift seen between Mach 1.70 and Mach 1.80. The lift then continues to drop as the velocity increases and the reflected shock waves strengthen. The lift is predicted to only increase again once these reflections have moved further downstream and the shock system under the aerofoil stabilises. This prediction is based on the gradually increasing lift performance of the h/c = 1.0 aerofoil between Mach 1.55 and Mach 2.00. Here, the shock system directly under the aerofoil remains relatively constant, as the shock interactions and reflections have moved downstream of the trailing edge of the aerofoil and no longer impact on the lift being produced.

In each case there is a complex interaction between the shock waves coming off the body and the reflected shocks propagating under and downstream of the aerofoil. These

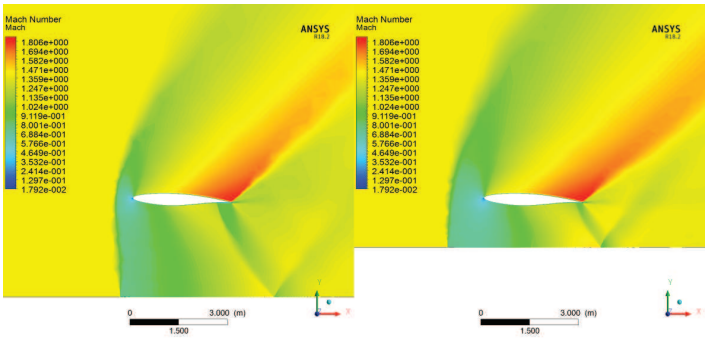

Mach 1.40

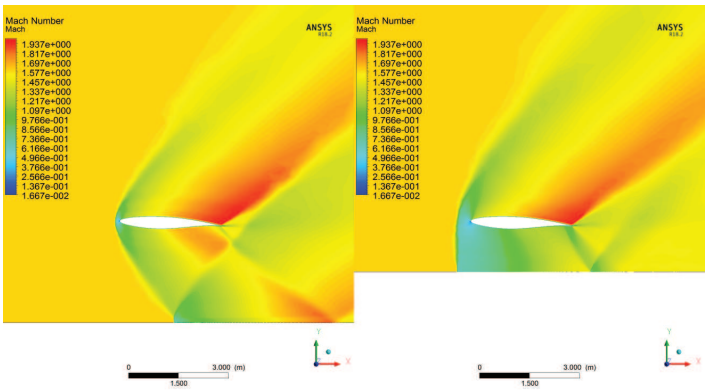

Mach 1.60

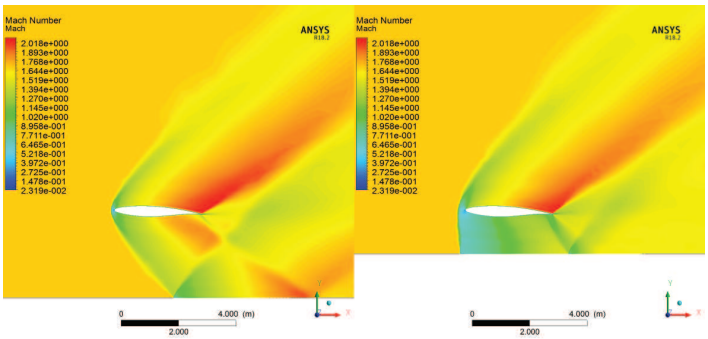

Mach 1.70

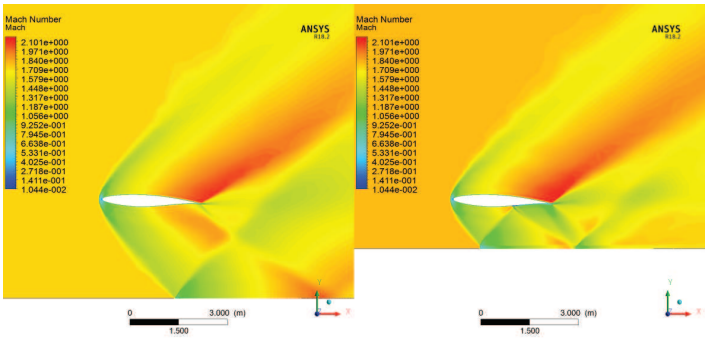

Mach 1.80

Fig.5 Comparison of the h/c = 1.0 (left) and h/c = 0.5 (right) steady state Mach number contour plots from Mach 1.40 to 1.80

interactions result in multiple regions of transonic and supersonic flow, especially as the reflected shock waves approach the compression waves and shear layer behind the aerofoil. With reference to Mach 1.60, 1.70 and 1.80 contours plots for the h/c = 1.0 in Figure 5. It appears that the reflected shock wave is not strong enough to pass through the region of compression waves and a weaker oblique shock forms underneath this region to rotate the flow accordingly. These interactions are further complicated in the h/c = 0.5 case, as multiple reflections occur underneath the aerofoil.

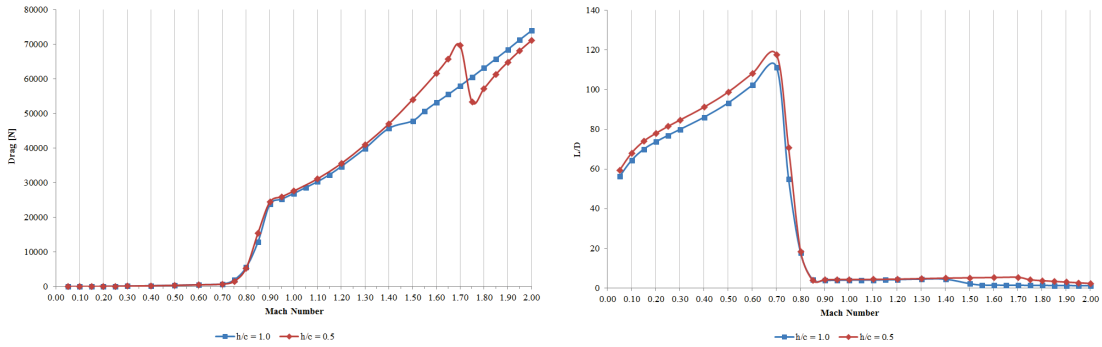

Fig.6 Drag performance (left) and aerodynamic efficiency (right) curves for an RAE 2822 aerofoil at two different ground clearances: h/c = 1.0 and h/c = 0.5

The drag performance and aerodynamic efficiency curves for the two ground clearance cases are compared in Figure 6. Throughout the velocity range, the drag results follow the same trend and only differ significantly from Mach 1.40 onwards. This difference comes from the induced drag component and the initial divergence (from Mach 1.40 to Mach 1.70) consequently follows the same behaviour observed in the lift curves. However, at Mach 1.70, there is a sudden decrease in drag on the lower aerofoil. This decrease occurs as the high pressure region under the leading edge fails and the bow shock and subsequent shock reflections move underneath the aerofoil. The drag drops below that of the higher aerofoil and as the shock system under the aerofoil stabilises, it starts to increase at the same rate as the higher aerofoil. This behaviour suggests that the reflecting shock waves beneath the lower aerofoil results in a reduction in the overall wave drag.

Furthermore, it is evident that once the shock waves start to form on the aerofoil, the resulting wave drag severely impacts the aerodynamic efficiency of the aerofoil. In both cases, the efficiency drops from an average lift-to-drag ratio of 115 at M0.70 to about 4 at Mach 0.90. The aerodynamic efficiency improves slightly as the bow shock starts to move under the aerofoil and the lift increases. Once the bow shock reflects, the drag rise supersedes the rise in lift and the aerodynamic efficiency continues to drop as the velocity increases. By Mach 2.00, it drops to a ratio of 1.22 and 2.36 for the higher and lower aerofoil respectively. Throughout the range, the increased ground effect gives the lower aerofoil a slight edge in aerodynamic efficiency.

3.2 Transient Analysis

Transient results were then conducted to evaluate the influence of acceleration and flow history on the aerodynamic performance at each ground clearance. From the steady state and transient lift curves in Figure 7 and Mach number contour plots given in Figures 8

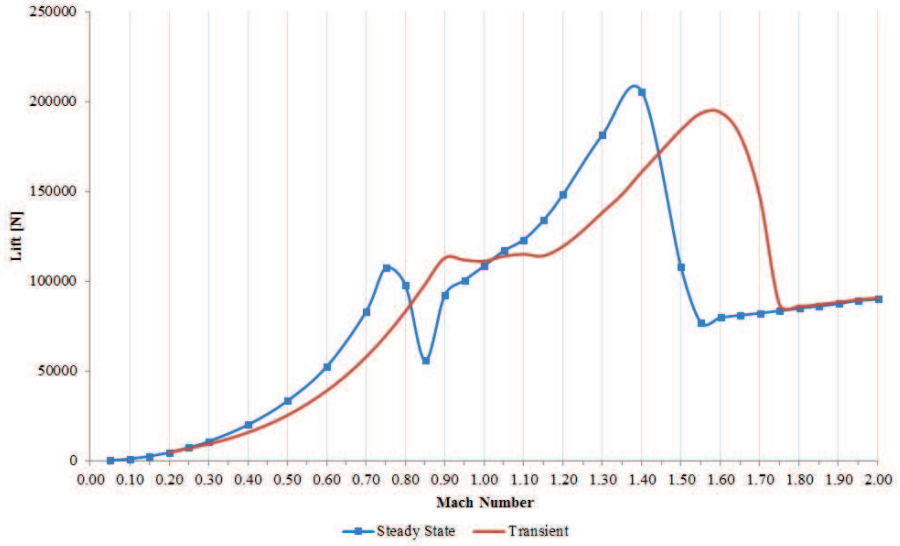

Fig.7 Steady state and transient lift curves for an RAE 2822 aerofoil at a ground clearance of h/c = 1.0

and 9: a distinct lag in the development of the transient flow can be seen. The lag can be seen from as early as Mach 0.30 and occurs as the flow is unable to fully develop and reach steady state as it accelerates. These undeveloped transient effects remain in the flow and impede the development of the flow as they move, develop and/or dissipate in the flow. This lag can also be seen in the shock formation, with the flow first becoming supersonic at critical Mach number of Mach 0.55 in the steady state and Mach 0.75 in the transient case.

The formation of shock waves below the aerofoil, can also be identified by the sudden changes in lift performance seen in each lift curve. In the steady state case, the lower shock forms under the aerofoil just after Mach 0.80 and reflects off the ground at Mach 0.90. The lift drops dramatically as the shock wave rapidly develops underneath the aerofoil. As illustrated in Figure 8, the same shock only starts to form at Mach 0.90 in the transient case and reflects off the ground at Mach 1.15 in Figure 9. The extreme acceleration of the flow, restricts the development and propagation of the transient shock wave under the aerofoil. Therefore, the shock takes longer to develop and cannot impart the same effects on the flow as the steady state case. This can be seen by the less dramatic fluctuations in the transient lift curve, as the shock forms between Mach 0.90 and Mach 1.15. Thereafter, the lift increases as the oblique shock coming off the inflection point stabilises and the pressure underneath the aerofoil starts to rise. This trend continues up until Mach 1.40 in the steady state case and Mach 1.65 in the transient, where the lift drops as the bow shock moves and reflects underneath the aerofoil. The movement and reflection of the bow shock under the aerofoil can be tracked by following the set of supersonic results in Figure 9. As the stand-off distance of the bow shock decreases, the angle of the bow shock increases and the bow shock starts to bend under the aerofoil. An pressure gradient starts to grow underneath the leading edge and eventually causes the bow shock to transition to a Mach reflection. The transition occurs just after Mach 1.40 and 1.65 for the steady and transient cases respectively.

The reflected bow shock propagates upwards, hits the lower surface of the aerofoil and

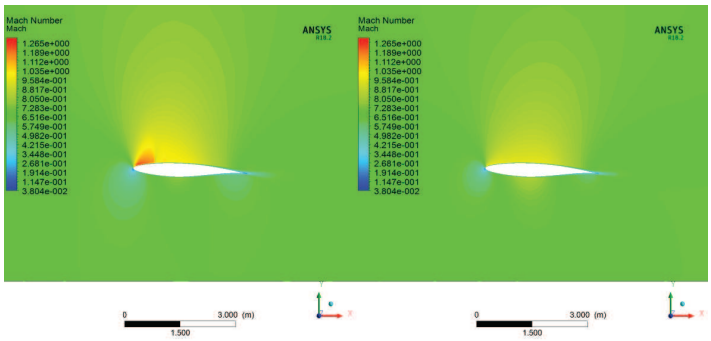

Mach 0.70

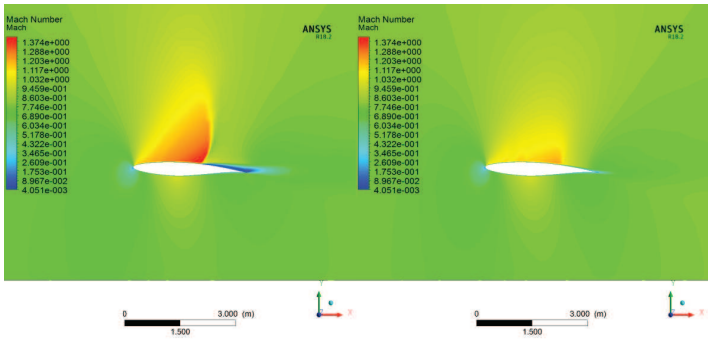

Mach 0.80

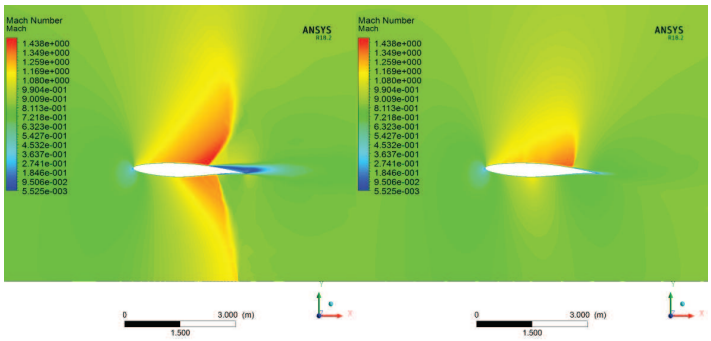

Mach 0.85

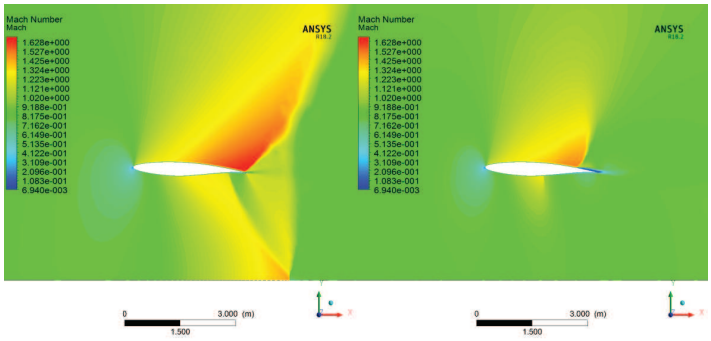

Mach 0.90

Fig.8 Mach number contour plot comparison of the lag between the steady state (left) and transient (right) transonic flow development

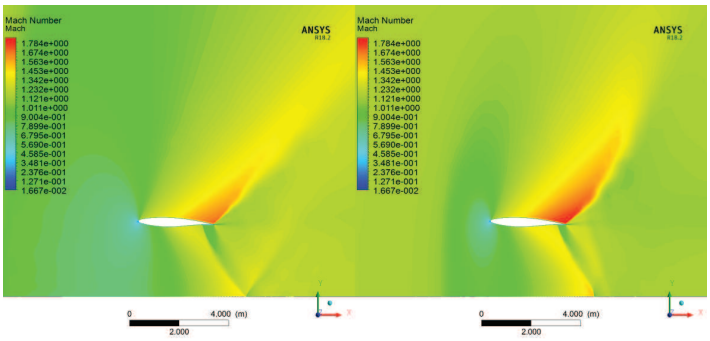

Mach 1.15

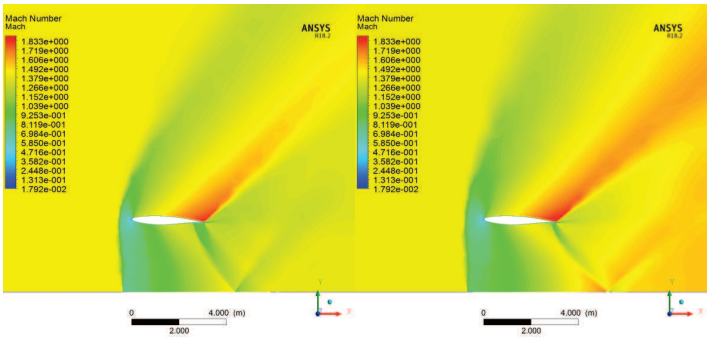

Mach 1.40

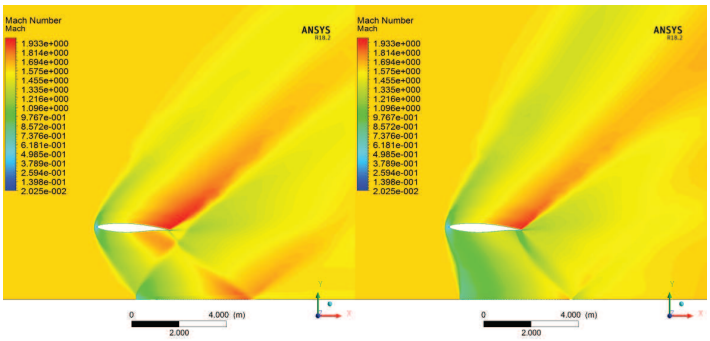

Mach 1.60

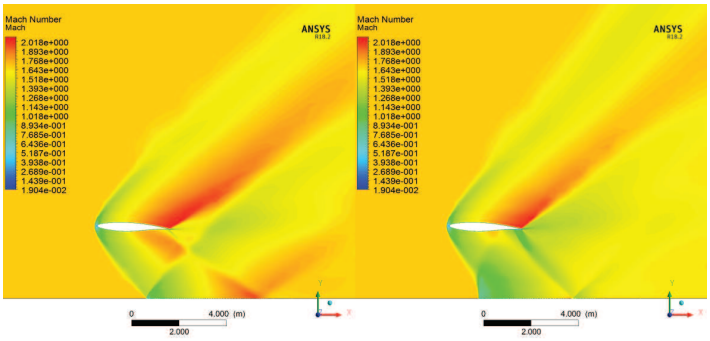

Mach 1.70

Fig.9 Mach number contour plot comparison of the lag between the steady state (left) and transient (right) flow development

then reflects back down towards the ground. This reflection moves further downstream as the flow develops and starts interacting with the oblique shock coming off the inflection point of the aerofoil. The interaction point then moves down and towards the trailing edge of the aerofoil. From Mach 1.60 in the steady state and Mach 1.80 in the transient case, this interaction moves aft of the trailing edge of the aerofoil and the shock structure under the aerofoil remains relatively constant. As a result, the lift is no longer affected by the downstream propagation and interaction of these shock waves and increases again at an almost linear rate. From Mach 1.80 onwards the steady state and transient results overlap. The transient flow under the aerofoil has overcome the undeveloped flow history effects and reaches steady state. Therefore, the transient and steady state conditions above and below the aerofoil are now similar and the lift results only vary by 1.45%. Figure 10 shows the similarity in the steady and transient shock systems at Mach 1.90 and Mach 2.00.

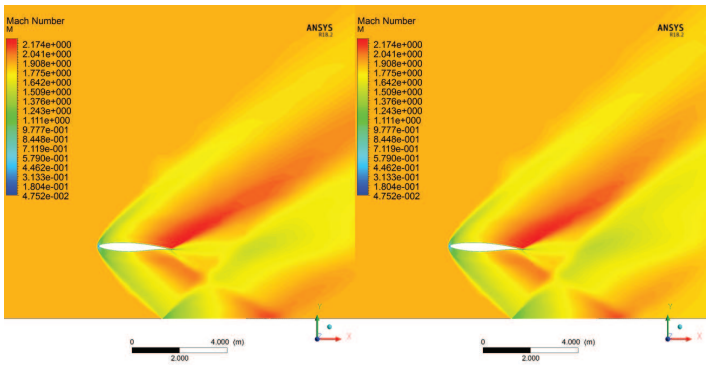

(a) Mach 1.90

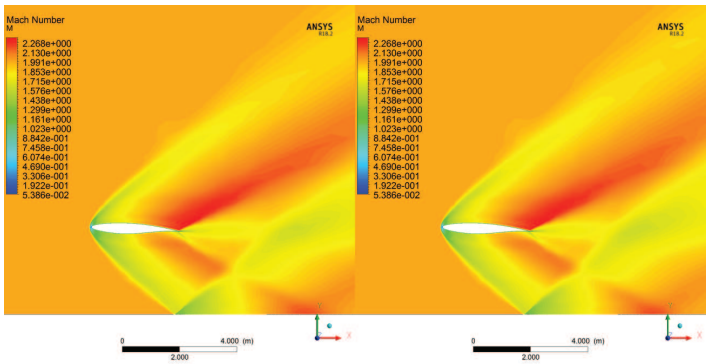

(b) Mach 2.00

Fig.10 Mach number contour plot comparison of similarities between the steady state (left) and transient (right) flow development at (a) Mach 1.90 and (b) Mach 2.00

The lag is less evident when comparing the steady state and transient drag results, given in Figure 11. However, it can be seen by the more gradual increase in wave drag between Mach 0.90 and 1.15 (as the lower shock forms underneath the aerofoil) and by the delayed drop off in drag that occurs at Mach 1.60 instead of at Mach 1.40 in the steady state case. An interesting development is that up until Mach 0.80, the transient drag is significantly higher than the steady state case. On average, the transient drag is 3.41 times greater during this range and reaches a maximum increase of 4.46 times greater

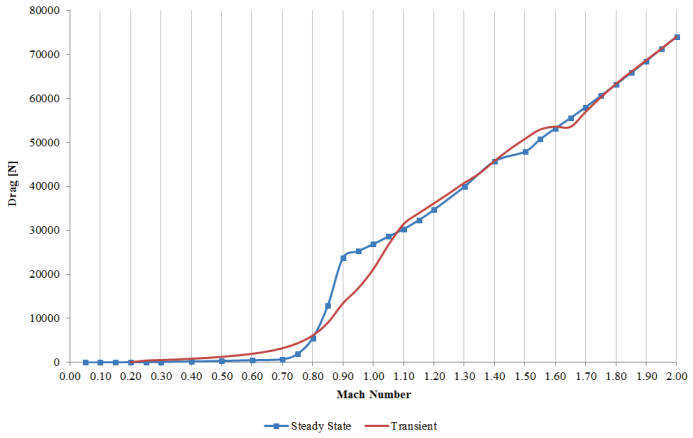

(a)

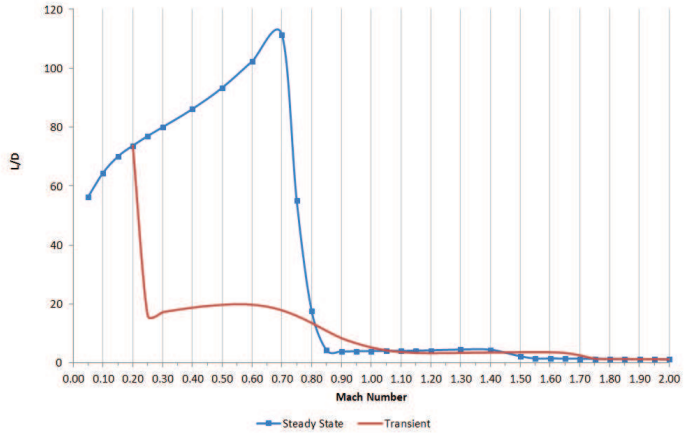

(b)

Fig.11 Steady state and transient drag (a) and aerodynamic efficiency (b) curves for an RAE 2822 aerofoil at a ground clearance of h/c = 1.0

at Mach 0.25. This increase in transient drag contrasts against the decrease in transient lift and results in a substantial drop in aerodynamic efficiency, as per Figure 11. The reason for this contrast is that as the transient results develop from the Mach 0.20 steady state case, the acceleration of the aerofoil is resisted by the inertia of fluid and the drag increases rapidly. Here, the inertia effects dominate the flow history effects seen in the lift results and only start to subside as the shock waves form on the aerofoil. Once the shock waves have formed above and below the aerofoil, the steady state and transient drag performance becomes similar and only differs as the induced drag component fluctuates with the lift results.

Overall, the transient shock wave development is less severe as the shock waves take longer to develop and propagate through the flow. Consequently, the transient shock waves are unable to fully develop and cause the same dramatic fluctuations seen in the steady state lift and drag performance. The transient shock development initially lags behind the steady state case by Mach 0.10, but as it takes longer for the transient shock to stabilise under the aerofoil, this lag extends to a difference of Mach 0.25. The flow is

unable to recover from this delay and the movement of the transient bow shock under the aerofoil is delayed by approximately the same amount. This delay results in a mismatch of the predicted lift for most of the considered velocity range, with the available lift being significantly over or under estimated at various points in the flow. The extent of this lag and significant difference in the steady state lift, shows the effects of flow history on the development of the flow and aerodynamic performance of the RAE 2822 aerofoil in tri-sonic ground effect.

The transient case for the lower ground clearance is also being investigated and should prove of interest, especially due to the more complex shock system that forms underneath the aerofoil and the combined effects of acceleration and ground effect. This investigation is further extended to evaluate the inertia and flow history effects on the down force produced by an inverted RAE 2822 aerofoil at a negative angle of attack of 2.79°. The effects of deceleration on these shock systems is also of interest, as the inertia effects would then oppose the drag force and flow history may have the opposite effect on the aerodynamic performance. Once this study is complete, an acceleration in the order of 3 g will be investigated to determine the impact of the flow history and inertia effects on the aerodynamic performance of a supersonic land speed vehicle.

4 Conclusions

The steady state and transient analysis reveal that ground effect and acceleration both delay the formation of shock waves on the aerofoil. This delay is then reflected in the aerodynamic performance of the aerofoil. As the shock waves form underneath the aerofoil, there is a subsequent drop in lift and increase in wave drag.

The delay in the ground effect results is caused by an increased pressure under the lower aerofoil, that eventually chokes the flow and prevents the bow shock from moving and reflecting underneath the aerofoil. The density and pressure of the choked flow increases under the lower aerofoil and leads to a maximum gain in lift of 460% at Mach 1.70. Once the bow shock reflects under the aerofoil, the lift drops dramatically and the lift behaviour of the two cases differs. This difference is a result of the different shock systems under the aerofoil. The lower aerofoil features another set of shock reflections under the aerofoil, that reduce the lift production of the aerofoil. In contrast, the reflected shock under the higher aerofoil stabilises and the lift steadily increases.

The delay in the transonic results occurs due to flow history effects, as the transient flow is unable to develop to the steady state conditions before reaching the next flow condition. Both flows develop the same shock waves and eventually the transient effects move down stream of the aerofoil and the transient flow above and below the aerofoil matches the steady state case. This occurs from Mach 1.75 onwards and there is a minimal difference in the aerodynamic performance of the two cases. Below this point the lag causes a substantial difference in the available lift predicted at each Mach number. Such differences in steady state and transient lift can potentially be dangerous if they are unexpected and left unaccounted for.

The steady analysis shows that ground effect has less of an impact on the drag performance of the aerofoil, with the only differences in drag coming from the induced drag component. Consequently, the aerodynamic efficiency is fairly similar, with the lower aerofoil featuring a slight advantage in aerodynamic efficiency throughout the range. However, the transient analysis reveals that acceleration has a significant impact on the subsonic and transonic aerodynamic efficiency of the aerofoil. Up until Mach 0.80, flow history

effects reduce the available lift and fluid inertia increases the drag at each Mach number. This results in a significant drop in the aerodynamic efficiency of the aerofoil, which severely impacts the performance and usability of the aerofoil under these conditions.

References

[1] B. Evans, C. Rose, *Simulating the aerodynamic characteristics of the Land Speed Record vehicle BLOODHOUND SSC*, Proc. IMechE Part D, J. Automobile Engineering, **228**, 10, pp. 1127-1141 (2014)

[2] H. Roohani, B. W. Skews, *Unsteady aerodynamic effects experienced by aerofoils during acceleration and retardation*, Proc. IMechE, Part G: J. Aerospace Engineering, **222(G5)**, pp. 631-636 (2008)

[3] H. Roohani, B. W. Skews, *The influence of acceleration and deceleration on shock wave movement on and around aerofoils in transonic flight.*, Shock Waves, **19**, 4 (2009)

[4] Vogt et al. *Flow Field Phenomena about Lift and Downforce Generating Cambered Aerofoils in Ground Effect*, Presented at the 16th Australasian Fluid Mechanics Conference (AFMC), **1**, pp. 328-335 (2007)

[5] Morrow et al., *The Effects of Rectilinear Acceleration on Shock Formation in Ground Effect*, Presented at the 23rd International Shock Interaction Symposium, University of the Witwatersrand (2018)

[6] Doig et al., *Aerodynamics of an aerofoil in transonic ground effect: numerical study at full-scale Reynolds numbers.*, The Aeronautical Journal, **116**, 1178 (2012)